On-line high-precision carbon position-specific stable isotope analysis - A review.

Caroline Gauchotte-Lindsay*, Stephanie M Turnbull

Infrastructure and Environment Research Division, School of Engineering, University of Glasgow, Rankine Building, Oakfield Avenue, Glasgow, UK, G12 8LT.

* Corresponding author: Email: caroline.gauchotte-lindsay@glasgow.ac.uk, Tel: 0141 330 3842

Abstract

Since the first commercial availability of gas chromatographs coupled with a combustion furnace and an isotope ratio mass spectrometer in 1990, compound specific stable isotope analysis of organic molecules has been at the origin of scientific breakthroughs in a wide range of research fields. The presence of non-reacting atoms, however, can mask changes in molecular stable isotopic signatures; position specific isotope analysis (PSIA) is the study of *intra*molecular isotopic variations. After considering briefly the potential and prospect of this new level in isotopic studies, we review here the handful of existing custom-built systems for on-line PSIA using continuous flow isotope ratio mass spectrometry instrumentation and how researchers have addressed issues specific to the technique. We also discuss the various molecular fragmentation processes observed and optimised for various molecules for on-line PSIA as it should help to inform application to new compounds.

Abbreviations

GC, Gas chromatography; GC-c-IRMS, Gas chromatography coupled with combustion furnace and isotope ratio mass spectrometry; BSIA, Bulk stable isotope analysis; CSIA, Compound specific isotope analysis; PSIA, Position specific isotope analysis; IRMS, Isotope ratio mass spectrometry; CF, Continuous flow; NMR, Nuclear magnetic resonance; SNIF-NMR, Site specific natural isotope fractionation nuclear magnetic resonance; EA-IRMS, Elemental Analysis - Isotope Ratio Mass Spectrometry; GC-Py-IRMS, Gas chromatography-pyrolysis-isotope ratio mass spectrometry; FID, Flame ionisation detector; FAMEs, fatty acid methyl esters; MTBE, methyl *tert* butyl ether; f, remaining fraction of reactant; KIEs, Kinetic isotope effects; AKIE, Apparent kinetic isotope effect; UVA, ultra violet

Keywords
Gas chromatography coupled with isotope ratio mass spectrometry; Bulk stable isotope analysis; Compound specific isotope analysis; Position specific isotope analysis; Isotope ratio mass spectrometry; Fluxomics

1 Introduction

There are three levels of specificity for stable isotope analysis: bulk stable isotope analysis (BSIA) [1], compound specific isotope analysis (CSIA) [2] and position specific isotope analysis (PSIA) [3] (Table 1). Historically, for isotope ratio analysis, the samples were quantitatively converted off-line to simple gases (CO_2 or CO and N_2 for carbon and nitrogen analysis and H_2 and CO for oxygen and hydrogen analysis) and then introduced to an isotope ratio mass spectrometer (IRMS) via an introduction system called dual-inlet. In the IRMS, the isotopic signatures were compared to calibrated gas standards. Dual-inlet analysis allows very precise and accurate stable isotope ratio analysis but requires large volumes of sample and tedious pre-analysis sample treatments [3]. The development of the continuous flow introduction system (CF) has enabled the direct analysis of much smaller sample volumes [3, 4]. The carrier gas (helium) carries the analyte in the gaseous phase into the ion source of the mass spectrometer. It has allowed the connection of IRMS to different automated sample preparation devices.

The magnitude of isotopic fractionation is greatest at the site of reaction in the molecule [5] and it has been accepted for a long time that *intra*molecular isotopic distribution was not homogeneous [6]. Position specific isotope analysis (PSIA) is the term that refers to the study of *intra*molecular isotopic variations within a molecule. Abelson and Hoering [7] presented the very first study on *intra*molecular isotopic variations. Using the nihydrin reaction, they performed the decarboxylation of several amino acids, collected the liberated CO_2 and measured its carbon stable isotope ratios by dual-inlet IRMS. The carboxyl groups showed great variability in function of the origin of the amino acids and in most cases were greatly enriched compared to the rest of the molecule. For the first time, the non-homogeneous isotopic distribution inside a molecule was revealed and the relationship between the origin of the molecule and the *intra*molecular isotopic variations was demonstrated. Abelson and Hoering also established that for PSIA, the reaction breaking down the molecule had to be

quantitative (total) so the isotope ratios of the fragments are representative of the moieties in the parent molecule. Although the off-line isolation of functional groups of interest by chemical reaction (chemolysis) provides precise intramolecular isotope analysis, it has not been widely used since Abelson and Hoering [7]. The few existing PSIA studies, however, consistently demonstrated that the carbon isotopic distribution in a molecule was heterogeneous and depended on its origin [6, 8]. Nuclear magnetic resonance (NMR) has also been used to determine site specific isotope signatures. The technique called site specific natural isotope fractionation nuclear magnetic resonance (SNIF-NMR) enabled to directly access site specific isotope ratio by identification and quantification of isotopomers by NMR [9]. It is widely used to determine D/H [10] ratios but has also been used for the determination of $^{13}C/^{12}C$ ratios [11]. Both off-line chemical reactions and NMR for position specific isotope analysis require a pure sample and therefore necessitate complicated extraction prior to analysis in very large sample sizes for accurate measurements [5]. NMR is however capable of producing results which are now comparable in accuracy to *intra*molecular isotope composition results obtained via IRMS analysis [5, 12].

Various reviews have extensively presented the wide range of the applications of CSIA ranging from archaeology to sport and including geo and extra-terrestrial chemistry, forensic and biomedical sciences [4, 13]. And in the same manner as CSIA greatly enhanced the resolution power of stable isotope analysis compared to BSIA, PSIA is the next resolution level. Brenna *et al.* [14] demonstrated in a review how natural *intra*molecular isotope measurements could help advance the field of physiology alongside other emerging techniques such as genomics and proteomics. Elsner *et al.* [15] identified PSIA as the next level of analysis for mechanistic isotopic fractionation studies of organic contaminants while Burton *et al*. [16] propose the use of the technique to identify the origin of the various carbon atoms in extra-terrestrial amino acids.

CF technologies enabled the development of on-line CSIA systems, which in turn triggered a rapid expansion of the method and its applications. On-line preparation of samples for PSIA using CF-IRMS is therefore theoretically possible too. However, while hyphenated IRMS instrumentations for on-line CSIA [2] have been available commercially since 1990 and are now widely employed, only a handful of laboratories carry out on-line PSIA for stable carbon isotope analysis on custom-built CF-IRMS instrumentations. In this review our aim is to introduce online-PSIA and

encourage further developments of this high-potential technique. To this aim, after discussing some current examples of PSIA applications and the potential of the technique as complementary to CSIA, we will present the existing CF-IRMS systems and their specific characteristics, advantages and drawbacks and inventory and categorize the reported mechanisms of on-line gaseous thermolysis of various compounds for on-line PSIA. This will also include discussions on how, for different systems and different fragmentation mechanisms, general issues such precision and sensitivity and issues more specific to PSIA such as isotopic fractionation and representativeness have been addressed.

2 Basics in position specific stable isotope analysis

We present here an overview of the fundamentals in stable isotope analysis at natural abundance level necessary to the understanding of this review, more detailed information can be found elsewhere (see for instance[1]).

The abundance of a stable isotope of an element, or the probability that an atom is of a particular isotope among the population of a given element, is represented either by the ratio (R) or the fraction (F) between the concentrations of the heavy (H) and the light (L) isotopes (Equation (1)).

$$R = \frac{H}{L} \text{ and } F = \frac{H}{L + H} \quad (1)$$

Isotope ratios, however, are conventionally expressed in delta (δ) notations relative to an international standard to facilitate inter-laboratory comparisons. They are relative values where the isotopic composition of a sample is compared to the isotopic composition of the standard and they are expressed in per mil (‰) (Equation (2)).

$$\delta H = \left(\frac{R_{\text{sample}} - R_{\text{standard}}}{R_{\text{standard}}}\right) \times 1000 \quad (2)$$

Chemical reactions, natural or anthropogenic, change the isotopic distribution of a molecule. It is predicted by statistical models that lighter isotopes form weaker bonds and therefore are more reactive than the heavier isotopes [5]. Consequently, the rate of a chemical reaction will be slower for molecules in which one of the atoms of the reactive bond is a heavy isotope; in general, this implies that the products of a reaction will contain a higher concentration of the lighter isotope, while reactants will be concentrated in the heavier isotope [5]. The change in relative abundances of stable

isotopes of an element due to a mass discriminatory process is termed isotopic fractionation. In a closed reversible system where the source of reacting substrate is not renewed the fractionation factor, α, is defined as the ratio of the R values of the products formed in an infinitely short time over that of the reactant. The kinetic isotope effects (KIEs) describe the ratios in reaction rate constant between molecules with ^{12}C and ^{13}C at the reactive position.

The fractionation factor, the remaining fraction of reactant (f) and the change in isotopic signature of the reactant during the reaction are all linked by the Rayleigh equation, an adaptation of Lord Rayleigh's equation on the fractionation of two compounds during distillation (Equation (3)[17]):

$$\ln\left(\frac{\delta H + 1000}{\delta H_0 + 1000}\right) = (\alpha - 1)\ln f = \frac{\varepsilon}{1000}\ln f \qquad (3)$$

With δH_0 the isotopic signature of the reactant before the start of the reaction and ε, equal to 1000(α-1) the enrichment factor.

.

The enrichment factor of a reaction can be determined experimentally through linear regression of $\ln(\delta H+1000/\delta H_0+1000)$ versus ln(f) in a controlled reaction.. It can then be used to calculate a value coined by authors [18] the apparent kinetic isotope effect (AKIE) using the following equation (Equation (4)):

$$AKIE = \frac{}{1 + z\frac{x}{1000}} \qquad (4)$$

n is the number of carbon atoms in the reacting molecule, with x of them are located at the site of reaction amongst which z are isotopically equivalent position. For primary isotope effect z=x. The term (n/x)ε is called the intrinsic or position enrichment factor and is meant to correct for the dilution in the observed enrichment factor due to non-reacting positions; it is based on the assumption that isotopes are distributed evenly within molecules of a same compound. For detail calculations leading to Equation 4 please refer to the review by Elsner *et al* [15]. When several mechanisms are suspected for a given reaction, the AKIE can be calculated for each

possible pathway and compared to KIEs computationally calculated using the Streitwieser Semiclassical Limits model [5] for various bond breaking/forming reactions. Divergences between observed AKIEs and KIEs could therefore be attributed to the assumption that stable isotopic signatures are homogeneous within a molecule. PSIA has therefore the potential to give access experimentally to more accurate AKIEs.

3 Applications of PSIA

PSIA allows observing and quantifying non-random distributions within molecules at natural abundance levels. These distributions are a representation of the "history" of natural and synthetic compounds: their synthesis and further transformations. At compound level, internal variations might be diluted by unchanging ratios. PSIA, off-line, on-line and using NMR, can be employed in two principal ways; 1) to mechanistically study (bio)chemical reactions and elucidate pathways and 2) to infer origins of chemically identical molecules of various origins including possible adulteration. In the following section, without attempting to be exhaustive, we aim to present examples of published applications of PSIA and particularly of on-line PSIA in CF systems to demonstrate the usefulness and potential of the method.

3.1 Origin and source inference

Off-line PSIA methods and SNIF-NMR have been employed to investigate the origin of natural and synthetic compounds. Particularly, ^{2}H-SNIF-NMR has been a very successful method for the authentication of beverages and food [19]. It was even adopted by the European Union in 1990 as the official method for the control of the addition of sugars to wines pre-fermentation (or chaptalisation) ([19] and references therein); the difference in position specific D/H ratio in the methyl and methylene groups of the ethanol molecule permitting to differentiate between sugar-added and natural wines. It has also been employed for the provenancing of illicit drugs [20]. For instance, the molecule of heroin derived from the acetylation of morphine and out of the 23 hydrogen atoms in a molecule of heroin, 15 are of natural origin and 8 of

198 "synthetic" origin; accessing their isotopic signature separately permit at the same
199 time to gather information on geographical origin of the drug and the commercial
200 source of its synthetic additive [20]. Recently, SNIF-NMR was extended to atoms
201 other than hydrogen. Bussy *et al*. [21] demonstrated notably the potential of carbon
202 position specific stable isotope analysis for the fingerprinting of active pharmaceutical
203 ingredients as a "tag" to combat counterfeiting as it could capture differences between
204 batches, manufacturing processes or origin in raw products.
205 As discussed previously, on-line CF methods are more compatible with complex low
206 concentration samples but their use has so far been limited for PSIA. With an on-line
207 PSIA system described in Section 4 (System 3 in Section 4) Hattori *et al.* [22] used
208 on-line pyrolysis of acetic acid to compare the $\delta^{13}C$ of the carboxyl and the methyl
209 carbon atoms of acetic acid in fourteen vinegars of various origins [22]. Thirteen out
210 of the 14 samples, exhibited acetic acid with a methyl carbon depleted compared to
211 the carboxyl carbon reflecting their biological origin. The last sample, however,
212 showed homogeneous carbon signature for the two positions unveiling a possible
213 addition of synthetic acetic acid to the vinegar. Gilbert *et al.* [23], using the same
214 system, analysed the intramolecular carbon stable isotope values of ethanol in various
215 alcoholic beverages and demonstrated that while the addition of C_4-based ethanol to
216 C_3-derived liquors could be detected at molecular level, *intra*molecular values for the
217 methanol and methyl groups in the ethanol molecule were necessary to detect addition
218 to CAM-derived beverages.
219 Using amino acids from various commercial sources, Brenna *et al.* compared
220 intramolecular isotopic variations with whole molecule variations [3]. Position
221 specific isotope analysis using System 4 (see Section 4) enabled to demonstrate that
222 the molecular variations were due to high variations at a restricted number of
223 positions [24]. PSIA also demonstrated that some of the amino acids from different
224 commercial distributors had the same sources or that a particular acid was not of
225 biological origin [24, 25].
226 Finally, on-line palladium catalysed decarboxylation of the low molecular weight
227 acids produced by hydrous pyrolysis of an oil-prone shale [26], in an early version of
228 System 2 (see Section 4), showed that while the $\delta^{13}C$ of the alkyl fragments of the
229 acids reflected the original kerogen, the $\delta^{13}C$ of the carboxyl carbon was an indication
230 of the isotopic signature of the dissolved inorganic carbon; experimentally proving

that the carboxyl carbon in organic acids in readily exchanged with aqueous inorganic carbon.

3.2 Mechanistic study of chemical reactions

The occurrence of isotopic fractionation during chemical reactions means that stable isotope can be employed to elucidate mechanistic pathways of reactions [27]. These fractionations are the greatest on the reacting atoms and the KIE on this given position will provide important clues on the nature and therefore the pathway of the reaction. KIEs are not accessible using CSIA and while multiple isotope enrichment factors can sometimes be useful; the method is limited for mechanistics studies.

In its simplest form PSIA can be used to investigate the pathway of a single chemical reaction. Oba and Naraoka [28], using a CF-IRMS system similar to System 2 (see Section 4), characterised the ultra violet degradation (UVA and visible) of acetic acid by looking at the changes in $^{13}C/^{12}C$ of both the whole molecule and the two carbon positions (the carboxyl carbon and the methyl carbon). PSIA on the acetic acid showed that the isotopic fractionation seen on the whole molecule was mainly attributable to fractionation on the carboxyl carbon, demonstrating that UV exposure might have a notable effect on the carbon stable isotope value of acetic acid present in carbonaceous meteorites. They were also able to determine the position specific enrichment factor values for the carboxyl, which could provide more detailed information on the mechanism.

Similarly, Gauchotte *et al.* characterised the permanganate oxidation of methyl *tert* butyl ether (MTBE), a gasoline oxygenate and ubiquitous groundwater contaminant by on-line PSIA, using System 5 (see Section 4)[29]. This enabled to simultaneously obtained $\delta^{13}C$ values for the two reactive groups in MTBE: the methoxy group and the 2-methylpropyl group. Firstly, before reaction the carbon atom of the methoxy group was found to be highly depleted compared to the 2-methylpropyl group, showing that in MTBE the distribution of ^{13}C is non statistical. Secondly, after about several hours of reaction, the $\delta^{13}C$ of whole molecule MTBE was enriched by 6.2‰, the $\delta^{13}C$ of the 2-methylpropyl group remained unchanged and the $\delta^{13}C$ of the methoxy group was enriched by 22.8‰ (Figure 2) demonstrating unequivocally that the C-H bonds of the methoxy group are the specific sites of this oxidation [29, 30] This had been the putative reaction pathway but had never been experimentally demonstrated.

Non-statistical distribution of ^{13}C in a molecule means that the assumption that the position specific enrichment factor is nε is usually incorrect and that AKIEs calculated using Equation (4) will often be inaccurate. A more appropriate value for the intrinsic enrichment factor should be $(\delta^{13}C_{total}/\delta^{13}C_{position})$ nε, but this is only accessible through PSIA analysis.

CSIA has become a very valuable tool over the last couple of decades for the evaluation of the fate of organic contaminants in the subsurface and several excellent reviews have been published in the last ten years [31-33], some focusing particularly on MTBE [18] an exemplar molecule for the technique. Authors have attempted to use CSIA results and particularly whole molecule enrichment factors, determined in laboratory microcosms [32], to calculate AKIEs and estimate new enrichment factors for different contaminants undergoing the same biodegradation process. This was because, as pointed out earlier, theoretically KIEs only depend on the local reaction mechanism and not the nature of the whole molecules. Attempts to experimentally demonstrate the conservation of the AKIEs, however, were not successful [34]. Morasch *et al*. presented a study of the anaerobic degradation of m-cresol and p-cresol by *D. cetonicum* on one hand, and of m-xylene and o-xylene by a strain OX39 on the other hand [34]. Both bacterial degradation pathways proceed *via* the formation of benzylsuccinate, with the first step of degradation being a hydrogen substitution on a methyl group of the substrate. All the carbon enrichment factors determined in this study were of the same order of magnitude. When the intrinsic or position specific enrichment factors were calculated, however, they were found different for each contaminant although the first step of reaction was identical. There are several possible reasons that explain these results. The first possible reason is the likely inaccuracy of nε as a value for the intrinsic enrichment factor. But an additional and important possibility is that enzymatic reactions cannot be directly assimilated to chemical reaction in terms of fractionations: there might additional rate-limiting steps such as 1) uptake and migration of compounds in the cell as demonstrated for instance by Nijenhuis *et al* [35]. through the comparison of enrichment factors associated with tetrachloroethylene dechlorination in pure cultures, cell free extracts and pure enzymes, 2) the commitment to catalysis (a measure of the efficiency of the enzymatic reaction) as defined by Northrop [36]and illustrated for example for the biodegradation of chloroethane by Lollar *et al.*[37] or else 3) the substrate-specificity of the reaction with differences in transition states as proposed by Rosell *et al.* in a

study of the biodegradation of different gasoline oxygenates [38]. Intrinsic enrichments for enzymatic reactions could be accessible only through PSIA.

Additionally, when looking at metabolites that are the products of a multi-enzymes metabolic pathway, the stable isotope signatures reflect multiple sequential isotope effects and their precursors. Bayle *et al*. [39] employed ^{13}C NMR to track and explain the carbon position specific stable isotope distribution in ethanol molecules issued from three different fermentation pathways, showing that the final carbon stable isotope distribution in ethanol was dependent on the catabolism. This study [39] and other similar [12, 40] to this one have shown that position specific isotope distributions in metabolites are pathway-specific and have allowed identifying the rate-limiting steps of the pathways. Currently, ^{13}C isotopic labelling is recognised as the most efficient method for the emerging field of fluxomics: the quantitative study of intracellular fluxes [41]. Coupled with metabolomics, fluxomics attempts to explain cellular phenotype and is expected to have an important impact in particular in biomedical science by facilitating drug discovery [42]. The recent analytical developments in PSIA, however, promise development of fluxomics at natural abundance levels, eliminating the need for complex synthesis of expensive labelled substrates and permitting to investigate all positions simultaneously [42].

4 On-line PSIA systems

The two analytical solutions for PSIA are SNIF-NMR, which has been reviewed elsewhere [9, 40, 43], and on-line PSIA using CF-IRMS systems. Although the first on-line PSIA system was reported in 1997 [3], the technology is still in its infancy. There is no commercial system available and a handful of laboratories have modified classic CF systems (Elemental Analysis-IRMS (EA-IRMS) or GC-IRMS) for PSIA studies. They fall into two categories: the systems specific to carboxylic acids and the systems compatible with all volatile and semi-volatile compounds.

4.1 On-line site-specific isotope analysis of carboxylic acids.

Carboxylic acids have been the single most important family of interest in the development of site-specific isotope analysis. Therefore, out of the few reported automated on-line systems for position specific isotope analysis, two are concerned with the decarboxylation of acids and the direct measurement of $\delta^{13}C_{carboxylic}$. These

systems [26, 44] are based on the high temperature chemolysis of acids, which break down into two pyrolysates: an hydrocarbon and CO_2, *i.e.*, benzoic acid breaks down into benzene and CO_2 [44] and butanoic acid into propane and CO_2 [26].

On-line site specific systems developed by Oba and Naraoka [44], System 1 presented in Figure 1, and Dias *et al*. [26] are based on simple modification of classic stable isotope analysis instrumentation. Dias *et al*. modified a GC-c-IRMS by replacing the usual oxidisers in the combustion furnace [26] with small palladium wires as catalysts and adding a small amount of pure hydrogen into the helium stream before the entrance to the furnace. Of the two gases produced by the catalytic pyrolysis, only the CO_2 is carried to the mass spectrometer for $\delta^{13}C$ measurements. The method was coined gas chromatography-pyrolysis-isotope ratio mass spectrometry (GC-Py-IRMS). In a similar manner, Oba and Naraoka modified an EA-Py-IRMS set-up usually employed for bulk stable isotope analysis (BSIA) [44]. The oxidation reactor of the elemental analyser was replaced with a ceramic tube filled with ceramic granules and the tube was topped with platinum wire, thus replicating a pyrolysis furnace [44]. After the separation of the pyrolysates in a gas chromatography column, only the stable isotopic ratios of the formed CO_2 were measured. Dias *et al.'s* system was designed for low molecular weight organic acids that are compatible with gas chromatography and in the system several acids contained in the same mixture can be analysed in a single run [26] but other types of compounds cannot be analysed. In the most recent version of the instrument [45], System 2 on Figure 1, a switching system was placed at the outlet of the column so that the compounds could be directed either directly into the combustion furnace for compound specific analysis or to the catalytic pyrolysis furnace for PSIA. On the other hand, in System 1 only the site-specific isotopic values of solid acids could be determined and therefore only pure samples and not mixtures can be analysed [44]. While adapted to a certain type of analyses, these systems are not ideally adapted to low concentration complex samples.

4.2 On-line systems with analytical flexibility

Yamada *et al.* developed an on-line system originally for the study of acetic acid. In this system the combustion reactor was not modified [46] instead a deactivated fused-silica capillary housed in a 25cm long heated ceramic tube was placed between the split/splitless injector and the inlet of the capillary column in a GC-c-IRMS apparatus. All compounds entering the injector would simultaneously be pyrolysed and pyrolysis

363 temperatures could be varied. All the pyrolysis fragments or pyrolysates (as opposed
364 to only the carboxylic CO_2 in the previously described systems) were then separated
365 in the column and their stable isotope signatures were obtained by classic combustion-
366 IRMS. This set-up as first described was adapted only to the analysis of pure volatile
367 (low molecular weight) acids because there was no means for on-line purification of a
368 single compounds out of mixtures [46]. The authors developed an improved version,
369 System 3 in Figure 1, in which the pyrolysis furnace was placed after the capillary
370 column in a first GC and the pyrolysates were separated in a capillary column placed
371 in a second GC, before being directed to the combustion furnace [21]. The
372 *intra*molecular carbon stable isotopes ratios in acetic acid and ethanol have been
373 investigated with this system [22, 23]. The main disadvantage of this approach,
374 however, is the impossibility to formally identify pyrolysates.
375 Corso and Brenna, pioneers of on-line PSIA, were the first to present a system with
376 real analytical flexibility [3]. It was not designed for any particular application but to
377 be compatible with a wide range of volatile compounds of interest. This system,
378 System 4 on Figure 1, adapted from gas chromatography-pyrolysis-gas
379 chromatography (GC-Py-GC) as first described by Dhont (1961) [47] constitutes of a
380 first gas chromatograph coupled with an inert pyrolysis reactor, which is in turn
381 coupled with a hybrid GC-c-IRMS/ion trap mass spectrometer system. An automated
382 four-port three-way valve placed at the outlet of the first capillary column enables to
383 direct the flow toward either a flame ionisation detector (FID) or a pyrolysis reactor.
384 The FID is used for quantitative analysis of compounds of interest. A fourth port of
385 the valve attached to a second injector allows for direct pyrolysis of pure samples.
386 Similarly to the system of Yamada *et al.*, the pyrolysis reactor is a piece of
387 deactivated fused silica joining the two gas chromatographs through a high
388 temperature furnace and a heated transfer line on each side. Pyrolysis temperature can
389 be adjusted. Additionally, a four-port three-way valve directs the effluent from the
390 second capillary column to either the mass spectrometer for molecular identification
391 of the pyrolysates or to combustion furnace and the IRMS.
392 The high flexibility of the system stems not only from the fact that the breakdown of
393 the molecules of interest into smaller fragments is based on non-catalytic non-specific
394 pyrolysis but also that all these fragments can be both identified in the ion trap mass
395 spectrometer and analysed through the IRMS for isotopic signatures. This system has
396 been used to date for the study of standards of a variety of compounds: fatty acid

methyl esters (through the example of methyl palmitate) [3],fatty alcohol (through the example of 1-hexanedecanol) [48], n-alkanes, toluene [49], the analogues of four amino acids: leucine, methionine [24], alanine and phenylalanine [25] and an analogue of lactic acid [50].

Gauchotte *et al.* also presented a flexible on-line PSIA system [29], System 5 on Figure 1. While the set-up is similar to System 4, the design of the pyrolysis reactor is significantly different. It is constructed of a quartz tube embedded in a temperature-controlled furnace. At the inlet of the reactor a tee union joins the end of the first capillary column, the quartz tube and a secondary helium supply while at the outlet an open-split was placed to release some of the pressure due to the added helium flow. While in previous systems, the transit time of the sample in the pyrolysis reactor depended only on its dimensions and could not be varied separately from the flow rate in the first capillary column, in this reactor the transit time can be varied by modification of the flow of added helium; giving greater control on the pyrolysis process. The system is also equipped with a liquid nitrogen cryo-trap placed after the pyrolysis reactor to ensure that all pyrolysates are focused when entering the second GC. The system has been used for the study of intramolecular carbon isotope variations in MTBE [29, 30].

5 Fragmentation processes and isotopic representativeness.

The breakdown of molecules of interest for on-line site-specific isotope analysis has been conducted in all reported on-line PSIA systems by high temperature chemolysis. The main issues are therefore to identify what moiety or moieties in the parent molecule the fragments originate from and how their carbon stable isotopic signatures relate. Ideally, the conversion should be total (quantitative), each fragment should represent a “slice” of the parent molecule without rearrangement and should not be involved in secondary reactions as it will affect their isotopic ratios. In this case only, the isotopic signatures of the fragments and corresponding moieties would be strictly equal and isotopic representativeness would be total. In most reported cases, however, these conditions were not fulfilled. First, secondary reactions might start before the primary reaction is total, destructing the isotopic representativeness of the pyrolysates. Secondly, scrambling might occur affecting what Sacks and Brenna coined “the structural fidelity” of the fragments: “the extent to which the isotope ratio of a

fragment reflects the isotope ratio of a specific position or moiety in the parent compound"[24]. Minimising these various effects means that at optimal pyrolysis conditions, f is generally below one and this means that isotopic fractionation might exist between parents and fragments.

The fragmentation mechanisms for reported online PSIA applications fall under three main categories: simple fragmentation of small molecules, non-ideal fragmentation of small molecules and fragmentation of long chain molecules. Table 2 presents an exhaustive summary of reported on-line fragmentation of molecules for PSIA and in this section, we discuss these mechanisms and the different strategies employed to address the various issues highlighted above. It is expected that fragmentation of new compounds for novel on-line PSIA applications would fall within one of these categories.

5.1 Simple fragmentation of small molecules

Here, we defined "simple fragmentation" of a molecule as the straight-forward cleavage of covalent bonds. Structural fidelity of fragmentation is 100% but isotopic representativeness might be affected when fragments are involved in secondary pyrolysis reactions (further fragmentations or polymerisation) or by isotopic fractionation when, in the ideal fragmentation conditions, the reaction is not quantitative.

As discussed in Section 4, on-line thermal decarboxylation of acid lead to the formation of a hydrocarbon and CO_2. In these cases, only the $\delta^{13}C_{carboxylic}$ was experimentally determined while the $\delta^{13}C$ of the complementary hydrocarbon was deduced from a mass conservation calculation using $\delta^{13}C_{carboxylic}$ and the $\delta^{13}C$ of the whole molecule. The main factor affecting the isotopic representativeness of the reported PSIA values was therefore the yield of the decarboxylation reaction.

The decarboxylation reactions employed in both cases were different. Oba and Naraoka's reaction was based solely on thermal decomposition [44]. For the three studied aromatic carboxylic acids, the reaction appeared to be at first a simple breakdown of the bond between the carboxylic carbon atom and the rest of the molecule thus forming CO_2 (Table 2). At high temperatures however, carbon

463 monoxide (CO) was also formed competing with the formation of CO_2 and therefore
464 changing the $\delta^{13}C_{carboxylic}$ value. To determine optimal temperature, the relative
465 amount of CO_2 (*i.e.* the intensity of the signal of the major ion 44) and the $\delta^{13}C_{carboxylic}$
466 (VPDB) were monitored at various temperatures. In all cases the maximum yield for
467 the production of CO_2 was reached at around 750°C and at higher temperatures the
468 amount of CO_2 started decreasing. On the other hand, the $\delta^{13}C_{carboxylic}$ values
469 presented a sigmoid curve in function of the temperature, the initial increase explained
470 by the kinetic isotope effect of the pyrolysis reaction before it reached completeness
471 and the second trend, starting when the amount of CO_2 started to decrease [44] due to
472 the secondary formation of the isotopically lighter CO. While the optimal temperature
473 for the pyrolysis appeared to be 750°C, there was no evidence that at this temperature
474 the conversion from the parent molecule to the CO_2 was quantitative and therefore
475 that the measured $\delta^{13}C$ value for the CO_2 was exactly equal to that of the parent
476 carbon atom in the acid. The accuracy of the obtained $\delta^{13}C_{carboxylic}$ was tested by three
477 different approaches. First, it was measured for various injected quantities of the
478 parent compounds and did not appear to vary. Then a liquid acid with known
479 $\delta^{13}C_{carboxylic}$ was analysed through the system and the measured value statistically
480 matched the accepted known value [44]. Finally, the $\delta^{13}C_{carboxylic}$ values of the acids
481 standards were determined by conventional off-line methods and the results were
482 within 1.0‰ of each other. The obtained stable isotopic values measured by the on-
483 line system could be deemed representative of the actual moiety values.
484 The thermal decarboxylation process used within the GC-Py-IRMS [26] followed a
485 different mechanism as it was helped by the addition of dihydrogen and catalysed by
486 palladium [51]. In this case also, the optimal temperature for the pyrolysis was
487 assumed to be the temperature for which the production of CO_2 was maximal
488 (600°C), however, there was no evidence that the reaction was complete or that
489 secondary reactions did not take place. The isotopic representativeness was partially
490 established by comparison of the results for two unlabelled carboxylic acids with the
491 GC-c-IRMS results of isotopic-dilution linear regressions for two acids with, ^{13}C
492 enriched carboxylic positions [26].
493 Yamada *et al.* also reported non-catalysed decarboxylation of acetic acid, producing
494 two main fragments: CO_2 and methane [46]. Other pyrolysis products were also
495 identified such as ethane and propane, which were most likely formed from the
496 polymerisation of methane. The carbon stable isotope ratios of all fragments was

497 measured. Comparison of the $\delta^{13}C$ values for CO_2 and methane with the $\delta^{13}C$ values
498 of the two parent moieties determined by off-line PSIA demonstrated that for a
499 pyrolysis temperature of 1000°C while the carbon isotopic value of CO_2 was similar
500 to $\delta^{13}C_{carboxylic}$, the $\delta^{13}C$ value of methane was depleted by almost 3‰ compared to
501 $\delta^{13}C_{methyl}$. This was possibly because methane was involved in secondary reactions.
502 To overcome the problem associated with the isotopic fractionation due to secondary
503 reaction, the $\delta^{13}C_{methyl}$ values were deduced from the subtraction of the $\delta^{13}C_{carboxylic}$
504 from the bulk isotopic value of the acetic acid [46].
505 Gilbert *et al.* [23] optimised the pyrolysis of ethanol. It was shown to occur through
506 two reactions: a dehydration producing ethylene and water and the breakdown of the
507 central C-C bond to form methane and CO. Using 14 different ethanol samples for
508 which the *intra*molecular distribution had been determined through an off-line
509 method, it was shown that for the breaking of the C-C bond, the CO fragment was
510 always depleted compared with the original moiety in the ethanol molecule while the
511 methane fragment was always enriched. The enrichment, and hence the fractionation
512 appeared, however, constant in all 14 samples which enabled to establish correction
513 factors and to obtain $\delta^{13}C_{VPDB}$ values of the two moieties. The authors also
514 demonstrated that the observed ethylene did not originate solely from the dehydration
515 reaction but also from the polymerisation of methane and therefore should be ignored
516 for PSIA of ethanol.
517 The on-line pyrolysis of toluene in System 4 [49] presented two fragments: benzene
518 and methane. The pyrolysis reaction was a simple cleavage of the C-C bond between
519 the benzene ring and the methyl group of the toluene as demonstrated by a ratio for
520 the peak areas of the major ion 44 of benzene and methane of 6:1 at 800°C. At this
521 temperature, the reaction yield was very low (Table 2). At higher temperature, the
522 (benzene: methane) ratio was lower due to secondary reactions on benzene. The
523 reconstituted $\delta^{13}C_{VPDB}$ value for toluene (calculated based on a Figure presented in
524 [49]) appears depleted of almost 3‰ compared to the measured $\delta^{13}C$ for the parent
525 molecule, demonstrating that isotopic fractionation occurred during the pyrolysis
526 reaction although it was not quantified by the authors.
527 In System 5, the gaseous on-line pyrolysis of MTBE produced isobutylene and
528 methanol via an intramolecular elimination breaking the C-O bond [29]. The pyrolysis
529 reaction was studied at both various temperatures and various pyrolysis reaction
530 times. Up to 675°C, the formation of the pyrolysates was equal to the consumption of

the parent molecule, but at higher temperatures and longer reaction times, the isobutylene and methanol concentrations were lower than that of the consumed MTBE, indicating the occurrence of secondary reactions. At the chosen optimal temperature for the pyrolysis reaction, the reaction was not total and therefore isotopic fractionation was expected. To evaluate the extent of the fractionation and correct the $\delta^{13}C$ values of the pyrolysates accordingly to obtain accurate $\delta^{13}C_{VPDB}$ for the two moieties, the carbon enrichment factor associated with the pyrolysis was measured using the Rayleigh equation (Equation 3). This allowed for a better understanding of the fractionation phenomena in the system. Two types of fractionations were identified. Firstly, a carbon isotopic shift of MTBE between the moment it enters the system and the pyrolysis was evidenced by the difference between the origin ordinate of the Rayleigh plot and the carbon isotopic signature of MTBE before pyrolysis. A first, pre-pyrolysis fractionation was measured. Secondly, using the measured enrichment factor for the pyrolysis, the kinetic isotopic fractionation of the pyrolysates was also calculated. Elucidation of the pyrolysis mechanism and of the two fractionations enabled to establish correction factors linking the carbon stable isotopic values of the pyrolysates to that of their parent moieties. The $\delta^{13}C$ values of the two MTBE functional groups could be reported against the international standard VPBD and isotopic representativeness established despite the occurrence of fractionation [29].

5.2 Non-ideal fragmentation of small molecules

The fragmentation of a small molecule is qualified as non-ideal when a fragment can be formed by two or more different pyrolysis reactions. Their carbon isotopic signature therefore does not represent the isotopic signature of a "slice" of the parent molecule but rather the mixing signatures from various positions and therefore their structural fidelity is smaller than 100%. For optimal PSIA, the level of structural fidelity of each fragment should be known. Brenna's team developed a method to measure fidelity for non-ideal fragmentation using isotopically labelled standards. In ideal situations a label standard should be used for each carbon position. The on-line pyrolysis of dilution series of these labelled standards is carried out and the fidelity of the various pyrolysates can be determined using the following equation (Equation (5)):

564 $$R_{fragment} = \sum_{i=1}^{n} R_i \xi_i = R_{lab} \xi_{lab} + \sum_{i=1}^{n-1} R_i \xi_i \quad (5)$$

565 Where n is the total number of carbon atoms in the parent molecule, $R_{fragment}$ is the
566 isotope ratio of a fragment, R_i, the isotope ratio and ξ_i, the fraction of carbon in the
567 product molecule originating from the position i, and R_{lab} and ξ_{lab} are the equivalent
568 value for the labelled position. The term sum of $R_i\xi_i$ is constant for each sample of a
569 dilution series. The slope of the linear regression of $R_{fragment}$ as a function of R_{lab} is
570 ξ_{lab}, the contribution of the labelled carbon atom to the fragment. For most reported
571 molecules (mainly amino acid derivatives) by Brenna *et al.* [24, 25, 50], the fidelity
572 was not 100% and the fragments were identified as originating from various carbon
573 atoms. When the fidelity of all the fragments has been determined, a system of
574 equations can be established. To calculate the isotopic values of n moieties in a
575 molecule, n equations are required, including the mass balance equation of the overall
576 molecule and n-1 equations for n-1 fragments including at least n-1 out of the n
577 carbon atoms. In certain cases, the fidelity might need to be determined at various
578 pyrolysis temperatures to obtain a sufficient number of equations.
579 In most cases, the fragments with the highest fidelity are formed at temperatures at
580 which the pyrolysis reaction is only partial and isotopic fractionation is therefore
581 likely to occur. Sacks and Brenna [24] proposed to report the isotopic ratios of the
582 fragments and the parent moieties in the sample (spl) relatively to a standard (std) of
583 the same molecule to cancel out the effect of the pyrolysis-induced fractionation using
584 $\Delta\delta^{13}C$ (spl) values (Equation (6)) [24]:
585 $$\Delta\delta^{13}C(spl) = \delta^{13}C(std) - \delta^{13}C(spl) \quad (6)$$
586 Indeed, the kinetic fractionation factor, α, from the pyrolysis reaction (Equation 3)
587 depends on parameter such as the temperature, the length of the furnace, the flow rate
588 but not on the original stable isotope ratios in the molecule and thus will be equal for
589 sample and standard.
590 Wolyniak *et al.* devised a method to estimate absolute *intra*molecular isotopic values
591 for molecules with complex pyrolysis processes through the example of the on-line
592 PSIA of propylene glycol [50]. The total fractionation, α, was first evaluated by
593 comparing the $\delta^{13}C$ of the parent compound to the average $\delta^{13}C$ of the fragments,
594 weighted by the fractional abundance of each fragment. Fragment specific
595 fractionation factors were then estimated by considering the possible scenarios of

fractionation, i.e. whether the fractionation happened on one carbon atom in the fragment or was equally distributed amongst the atoms. The $\delta^{13}C$ value of each fragment was then corrected for pyrolysis fractionation and a new system of equations was established using the new absolute isotopic ratio for the fragments and the same fidelity values and absolute values were obtained for the each of the three carbon atoms with a standard deviation of <3‰.

5.3 Pyrolysis of long chain molecules

Brenna *et al.* [1, 48, 49]carried out high precision position-specific isotope analysis on a series of aliphatic chain molecules: methyl palmitate, a fatty acid methyl esters (FAMEs), 1-hexanedecanol, a fatty alcohol and a series of the n-alkanes (n-pentane, n-hexane, n-heptane, n-octane and n-decane).

The long chain molecules fragmented by pyrolysis into two series of fragments that corresponded to the breaking of a single C-C bond along the chain: a ω-monounsaturated methyl ester series and the complementary olefins for methyl palmitate (Me 16:0) and alcohol series and the complementary olefin series for 1-hexadecanol. Carbon rearrangement during pyrolysis was ruled out by carrying out the on-line pyrolysis of compounds isotopically labelled at various positions [52]. The carbon isotopic signatures of the fragment containing the carboxylic or alcohol position follow the mass balance (Equation (7)):

$$F_T = \chi_{C1} F_{C1} + (1 - \chi_{C1}) F_R = \chi_{C1}(F_{C1} - F_R) + F_R \quad (7)$$

Where F is the ^{13}C fraction and χ the molecular fraction (T=total, C1= the carboxylic or alcohol position and R= all other remaining positions in the fragment). Thus, when plotting F_T in function of χ_{C1} assuming F_R constant, the y-axis intercept (F_R) corresponds to the mean isotope fraction of the molecule excluding the first position while the ^{13}C fraction of the carboxylic or alcohol position is obtained by slope+F_R. To validate this model for both the FAME and the fatty alcohol, high precision position-specific isotope analysis was carried out on a mixture of unlabelled compounds and [1-^{13}C] labelled compounds. The isotopic values for the olefins series were uniform and in the expected natural abundance range while the plots for the methyl ester/alcohol series carbon isotopic signatures as a function of the number of carbon atoms had the appearance of a mixing curve. The influence of the labelled position decreasing by dilution with the increase of the fragment molecular size. In

the case of methyl palmitate the value obtained for F_R matched closely the mean ^{13}C atomic fraction of the olefins series (excluding methane and ethylene) while the values obtained for F_{C1} corresponded to the value expected after the dilution of the labelled compound. In the case of the fatty alcohol, the correspondence between the calculated F_R value and the average ^{13}C atomic fraction for the olefins series presented a difference equivalent to around 6‰. This provided evidence of fractionation of the parent compound, which the authors attributed to the competing formation of a dehydration product present on the pyrolysates chromatogram.

The n-alkanes also broke down in complementary series [49]. Each alkane fragmented into a series of straight-chain hydrocarbons separated by one carbon unit ranging from the methane to the parent compound. The study of the peak area percentage of the alkane fragments presented evidence of secondary pyrolysis reactions that implied that the isotopic representativeness of the measurement was affected. To measure the overall discrepancy between the fragments isotopic signatures and the parent compound, Brenna *et al*. [49] proposed to calculate the mean of the weighed averages of the isotope ratios of complementary fragments (two fragments for which the combination of carbon atom numbers adds up to the number of carbon atoms in the parent molecule) and to compare it to the isotope ratio of the parent compound. For both the alkanes and the 1-hexanedecanol, this method unveiled small but statistically significant differences. These could be due to possible secondary reactions but also to the kinetic isotope effect of the pyrolysis, which in all cases was not quantitative. In fact, comparison of the pyrolysis fragments isotopic signatures at different pyrolysis temperatures [49, 52] divulged slight differences. While optimal pyrolysis temperatures were chosen to minimise the possibility of a secondary reaction, i.e. smaller yields, it meant that the kinetic isotope effect of the pyrolysis was more important but was not quantified.

6 Precision and sensitivity

On-line PSIA systems are part of the interface development that followed the invention of continuous flow IRMS systems. Continuous flow systems are less precise than dual inlet systems but have better sensitivity. In order to be successful continuous flow devices, PSIA systems must offer precision and sensitivity equivalent to other systems.

In most cases, when the pyrolysis is not complete, isotopic representativeness of the carbon isotopic values for the moieties (i.e. an accurate VPDB value) can be obtained only if the extent and the location of the isotopic fractionation are known. The reported precision is therefore usually the precision on the measured $\delta^{13}C$ value for the pyrolysates or for $\Delta\delta^{13}C$ (*spl*) and not for the $\delta^{13}C$ of the moiety in the parent compound. For most on-line PSIA systems, the instrumental precision is unchanged compared to a classic GC-c-IRMS (Table 3) and is around 1σ =0.4‰. Reported precision for $\Delta\delta^{13}C$ (*spl*) values in System 4 is similar. When attempting to account for the isotopic fractionation by theoretical calculations, Wolyniak *et al*. then reported a precision of 1σ <3.0‰ [25]. When correction factors were calculated between the $\delta^{13}C$ values of the pyrolysis products and that of the parent moiety using the Rayleigh equation of the pyrolysis, error propagation on the experimentally derived terms meant that the overall precision was a 95% confidence interval of 0.5‰ [29].

The sensitivity of PSIA system can be affected by three main factors: the number of carbon atoms in the fragment, the yield of the pyrolysis reaction and the addition of gas through the system. In most devices apart from System 5 the mass of gas through the system is not different to that of a classic GC-c-IRMS. When the pyrolysis reaction is quantitative the sensitivity should only be affected by the fact that the pyrolysates present a smaller amount of carbon atoms than the parent molecule and thus have a smaller IRMS signal [45]. The sensitivity is limited by the number of carbon atoms in the smallest fragment. For instance, if a molecule containing seven carbon atoms breaks down into on fragment containing five carbon atoms and one containing two carbon atoms, the sensitivity of on-line PSIA compared to CSIA of the same molecule will be decreased by 71% (2/7). In many cases, however, the optimal conditions for pyrolysis correspond to condition when the reaction is not total and f<1 (Table 2), which means that the sensitivity is further affected by the low production of pyrolysates. For instance, if for the same pyrolysis reaction, the remaining fraction of reactant at optimal temperature is 40% then the sensitivity is further decreased by 60% and the total loss of sensitivity is around 85%. Therefore, by the nature of the analysis on-line PSIA detection limits are higher than for classic CSIA systems presenting a clear limitation to the method. Reported precisions and sensitivity for existing systems are presented in Table 3.

7 Conclusions

PSIA has been identified by leading isotope researchers along with clumped isotopes as the future for isotopic research [53]. The applications of the technique span across a very wide range of topics. While in astrobiology it could help elucidate the origin of life on Earth in biochemistry it could become an invaluable tool to complement the emerging ‘omics approaches.

And while its potential was first unveiled several decades ago [7], the analytical difficulties intrinsic to the measurements notably in complex mixtures and at trace level have for a long time limited its development. PSIA techniques using CF-IRMS and SNIF NMR are now employed by a handful of laboratories and applications are multiplying. Tellingly, Yamada *et al.* [54] have now developed reference materials for acetic acid on-line PSIA studies in order to facilitate inter-laboratory and inter-method calibration; demonstrating a more routine future for the technique.

List of Figures:

Figure 1- On-line PSIA systems developed from CF-IRMS instrumentation. Systems 1 and 2 permit on-line decarboxylation of acids and provide direct measurements of the carbon stable isotope ratios of the carboxylic carbon atom. Systems 3, 4 and 5 are non-specific systems and have been employed for a wide range of organic compounds. The three systems are constituted of two GCs enabling the isolation of the compound of interest in the first GC and the separation and CSIA of its fragmentation compounds through the second GC. **a:** Pyrolysis chamber consisting of a ceramic tube containing deactivated fused silica, **b:** Pyrolysis chamber consisting of a ceramic tube containing ceramic granules with 30cm of platinum wire crumpled on top of the granules, **c:** Pyrolysis chamber consisting of a quartz tube with capillary column inserted into both ends of the tube, **d:** Pyrolysis chamber consisting of ceramic alumina tube filled with four palladium wires, **e**: Combustion furnace, **f:** 4 port Valco valve, **g:** GC column, **h:** Back flush system

Figure 2- Changes (Δ) in carbon stable isotope ratios of MTBE and its pyrolysates (methanol and isobutylene) in System 4 during permanganate oxidation of MTBE (Reproduced from [30]). The signature of the pyrolysate (isobutylene) representative of the non-reacting position remained unchanged while that of the pyrolysate representative of the carbon atom at the first site of attack (methanol) became greatly enriched.

List of Tables:

Table 1- Levels of specificity in stable isotope analysis.

Table 2- Fragmentation of organic compounds in on-line PSIA systems. The compounds are categorized by fragmentation mechanisms. [1]f is the remaining fraction of reactant at optimal fragmentation conditions. [2] 100% structural fidelity means that the isotope ratio of a fragment uniquely originates from the isotope ratio of a specific position in the parent compound. [3] System numbers refer to numbers presented in Figure 1. n.r.= non reported

Table 3- Reported precisions and sensitivity of the on-line PSIA systems. [1]

System numbers refer to numbers presented in Figure 1.

Acknowledgments

The authors would like to thank the EPSRC for financial support through grants EP/D013739/1 and EP/D013739/2, the Royal Society for the Paul Instrument Fund Fellowship granted to CGL and the University of Glasgow for SMT's PhD studentship.

Uncategorized References

[1] J.T. Brenna, T.N. Corso, H.J. Tobias, R.J. Caimi, High-precision continuous-flow isotope ratio mass spectrometry, Mass Spectrom Rev, 16 (1997) 227-258.
[2] W. Meier-Augenstein, Applied gas chromatography coupled to isotope ratio mass spectrometry, Journal of chromatography. A, 842 (1999) 351-371.
[3] T.N. Corso, J.T. Brenna, High-precision position-specific isotope analysis, Proceedings of the National Academy of Sciences, 94 (1997) 1049-1053.
[4] S. Benson, C. Lennard, P. Maynard, C. Roux, Forensic applications of isotope ratio mass spectrometry—a review, Forensic science international, 157 (2006) 1-22.
[5] L.C. Melander, W.H. Saunders, Reaction rates of isotopic molecules, Wiley New York1980.
[6] K.D. Monson, J.M. Hayes, Carbon isotopic fractionation in the biosynthesis of bacterial fatty acids. Ozonolysis of unsaturated fatty acids as a means of determining the intramolecular distribution of carbon isotopes, Geochimica et Cosmochimica Acta, 46 (1982) 139-149.
[7] P.H. Abelson, T.C. Hoering, Carbon Isotope Fractionation in Formation of Amino Acids by Photosynthetic Organisms, P Natl Acad Sci USA, 47 (1961) 623-&.
[8] T. Weilacher, G. Gleixner, H.-L. Schmidt, Carbon isotope pattern in purine alkaloids a key to isotope discriminations in C1 compounds, Phytochemistry, 41 (1996) 1073-1077.
[9] G.J. Martin, S. Akoka, M.L. Martin, SNIF-NMR—Part 1: Principles, Modern Magnetic Resonance, Springer2006, pp. 1651-1658.
[10] M.L. Martin, G.J. Martin, Site-specific isotope effects and origin inference, Analusis, 27 (1999) 209-213.
[11] V. Caer, M. Trierweiler, G.J. Martin, M.L. Martin, Determination of site-specific carbon isotope ratios at natural abundance by carbon-13 nuclear magnetic resonance spectroscopy, Analytical chemistry, 63 (1991) 2306-2313.

787 [12] A. Gilbert, R. Hattori, V. Silvestre, N. Wasano, S. Akoka, S. Hirano, K. Yamada,
788 N. Yoshida, G.S. Remaud, Comparison of IRMS and NMR spectrometry for the
789 determination of intramolecular 13C isotope composition: Application to ethanol,
790 Talanta, 99 (2012) 1035-1039.
791 [13] S. Asche, A.L. Michaud, J.T. Brenna, Sourcing organic compounds based on
792 natural isotopic variations measured by high precision isotope ratio mass
793 spectrometry, Current Organic Chemistry, 7 (2003) 1527-1543.
794 [14] J.T. Brenna, Natural intramolecular isotope measurements in physiology:
795 elements of the case for an effort toward high-precision position-specific isotope
796 analysis, Rapid Communications in Mass Spectrometry, 15 (2001) 1252-1262.
797 [15] M. Elsner, L. Zwank, D. Hunkeler, R.P. Schwarzenbach, A new concept linking
798 observable stable isotope fractionation to transformation pathways of organic
799 pollutants, Environmental science & technology, 39 (2005) 6896-6916.
800 [16] A.S. Burton, J.C. Stern, J.E. Elsila, D.P. Glavin, J.P. Dworkin, Understanding
801 prebiotic chemistry through the analysis of extraterrestrial amino acids and
802 nucleobases in meteorites, Chemical Society Reviews, 41 (2012) 5459-5472.
803 [17] A. Mariotti, J. Germon, P. Hubert, P. Kaiser, R. Letolle, A. Tardieux, P.
804 Tardieux, Experimental determination of nitrogen kinetic isotope fractionation: some
805 principles; illustration for the denitrification and nitrification processes, Plant and soil,
806 62 (1981) 413-430.
807 [18] L. Zwank, M. Berg, M. Elsner, T.C. Schmidt, R.P. Schwarzenbach, S.B.
808 Haderlein, New Evaluation Scheme for Two-Dimensional Isotope Analysis to
809 Decipher Biodegradation Processes: Application to Groundwater Contamination by
810 MTBE, Environmental Science & Technology, 39 (2005) 1018-1029.
811 [19] L.M. Reid, C.P. O'Donnell, G. Downey, Recent technological advances for the
812 determination of food authenticity, Trends in Food Science & Technology, 17 (2006)
813 344-353.
814 [20] S. Armellin, E. Brenna, S. Frigoli, G. Fronza, C. Fuganti, D. Mussida,
815 Determination of the synthetic origin of methamphetamine samples by 2H NMR
816 spectroscopy, Analytical chemistry, 78 (2006) 3113-3117.
817 [21] U. Bussy, C. Thibaudeau, F. Thomas, J.-R. Desmurs, E. Jamin, G.S. Remaud, V.
818 Silvestre, S. Akoka, Isotopic finger-printing of active pharmaceutical ingredients by
819 13 C NMR and polarization transfer techniques as a tool to fight against
820 counterfeiting, Talanta, 85 (2011) 1909-1914.
821 [22] R. Hattori, K. Yamada, M. Kikuchi, S. Hirano, N. Yoshida, Intramolecular
822 carbon isotope distribution of acetic acid in vinegar, Journal of agricultural and food
823 chemistry, 59 (2011) 9049-9053.
824 [23] A. Gilbert, K. Yamada, N. Yoshida, Accurate method for the determination of
825 intramolecular 13C isotope composition of ethanol from aqueous solutions, Anal
826 Chem, 85 (2013) 6566-6570.
827 [24] G.L. Sacks, J.T. Brenna, High-Precision Position-Specific Isotope Analysis
828 of13C/12C in Leucine and Methionine Analogues, Analytical Chemistry, 75 (2003)
829 5495-5503.
830 [25] C.J. Wolyniak, G.L. Sacks, B.S. Pan, J.T. Brenna, Carbon position-specific
831 isotope analysis of alanine and phenylalanine analogues exhibiting nonideal pyrolytic
832 fragmentation, Anal Chem, 77 (2005) 1746-1752.
833 [26] R.F. Dias, K.H. Freeman, S.G. Franks, Gas chromatography–pyrolysis–isotope
834 ratio mass spectrometry: a new method for investigating intramolecular isotopic
835 variation in low molecular weight organic acids, Organic Geochemistry, 33 (2002)
836 161-168.

837 [27] B.-L. Zhang, S. Buddrus, M.L. Martin, Site-specific hydrogen isotope
838 fractionation in the biosynthesis of glycerol, Bioorganic Chemistry, 28 (2000) 1-15.
839 [28] Y. Oba, H. Naraoka, Carbon and hydrogen isotope fractionation of acetic acid
840 during degradation by ultraviolet light, Geochemical Journal, 41 (2007) 103-110.
841 [29] C. Gauchotte, G. O'Sullivan, S. Davis, R.M. Kalin, Development of an advanced
842 on-line position-specific stable carbon isotope system and application to methyl tert-
843 butyl ether, Rapid Communications in Mass Spectrometry, 23 (2009) 3183-3193.
844 [30] C. Gauchotte, G. Connal, G. O'Sullivan, R.M. Kalin, Position Specific Isotope
845 Analysis: The Ultimate Tool in Environmental Forensics?, Environmental Forensics :
846 Proceedings of the 2009 INEF Annual Conference, RSC Publishing2010, pp. 60-70.
847 [31] T.B. Hofstetter, M. Berg, Assessing transformation processes of organic
848 contaminants by compound-specific stable isotope analysis, Trac-Trend Anal Chem,
849 30 (2011) 618-627.
850 [32] R.U. Meckenstock, B. Morasch, C. Griebler, H.H. Richnow, Stable isotope
851 fractionation analysis as a tool to monitor biodegradation in contaminated acquifers,
852 Journal of Contaminant Hydrology, 75 (2004) 215-255.
853 [33] T.C. Schmidt, H.-A. Duong, M. Berg, S.B. Haderlein, Analysis of fuel
854 oxygenates in the environment, Analyst, 126 (2001) 405-413.
855 [34] B. Morasch, H.H. Richnow, A. Vieth, B. Schink, R.U. Meckenstock, Stable
856 isotope fractionation caused by glycyl radical enzymes during bacterial degradation of
857 aromatic compounds, Appl Environ Microbiol, 70 (2004) 2935-2940.
858 [35] I. Nijenhuis, J. Andert, K. Beck, M. Kästner, G. Diekert, H.-H. Richnow, Stable
859 isotope fractionation of tetrachloroethene during reductive dechlorination by
860 Sulfurospirillum multivorans and Desulfitobacterium sp. strain PCE-S and abiotic
861 reactions with cyanocobalamin, Applied and Environmental Microbiology, 71 (2005)
862 3413-3419.
863 [36] D.B. Northrop, The expression of isotope effects on enzyme-catalyzed reactions,
864 Annual review of biochemistry, 50 (1981) 103-131.
865 [37] B.S. Lollar, S. Hirschorn, S.O. Mundle, A. Grostern, E.A. Edwards, G.
866 Lacrampe-Couloume, Insights into enzyme kinetics of chloroethane biodegradation
867 using compound specific stable isotopes, Environmental science & technology, 44
868 (2010) 7498-7503.
869 [38] M. Rosell, R. Gonzalez-Olmos, T. Rohwerder, K. Rusevova, A. Georgi, F.D.
870 Kopinke, H.H. Richnow, Critical evaluation of the 2D-CSIA scheme for
871 distinguishing fuel oxygenate degradation reaction mechanisms, Environ Sci Technol,
872 46 (2012) 4757-4766.
873 [39] K. Bayle, S. Akoka, G.S. Remaud, R.J. Robins, Non-Statistical 13C Distribution
874 during Carbon Transfer from Glucose to Ethanol During Fermentation is Determined
875 by the Catabolic Pathway Exploited, Journal of Biological Chemistry, DOI (2014)
876 jbc. M114. 621441.
877 [40] M. Martin, B. Zhang, G.J. Martin, SNIF-NMR—Part 2: Isotope Ratios as Tracers
878 of Chemical and Biochemical Mechanistic Pathways, Modern Magnetic Resonance,
879 Springer2006, pp. 1659-1667.
880 [41] S. Klein, E. Heinzle, Isotope labeling experiments in metabolomics and
881 fluxomics, Wiley Interdisciplinary Reviews: Systems Biology and Medicine, 4 (2012)
882 261-272.
883 [42] M. Cascante, S. Marin, Metabolomics and fluxomics approaches, Essays
884 Biochem, 45 (2008) 67-82.

885 [43] G.J. Martin, M.L. Martin, G. Remaud, SNIF-NMR—Part 3: From Mechanistic
886 Affiliation to Origin Inference, Modern Magnetic Resonance, Springer2006, pp.
887 1669-1680.
888 [44] Y. Oba, H. Naraoka, Site-specific carbon isotope analysis of aromatic carboxylic
889 acids by elemental analysis/pyrolysis/isotope ratio mass spectrometry, Rapid
890 Communications in Mass Spectrometry, 20 (2006) 3649-3653.
891 [45] B. Thomas, K.H. Freeman, M.A. Arthur, Intramolecular carbon isotopic analysis
892 of acetic acid by direct injection of aqueous solution, Organic Geochemistry, 40
893 (2009) 195-200.
894 [46] K. Yamada, M. Tanaka, F. Nakagawa, N. Yoshida, On-line measurement of
895 intramolecular carbon isotope distribution of acetic acid by continuous-flow isotope
896 ratio mass spectrometry, Rapid communications in mass spectrometry : RCM, 16
897 (2002) 1059-1064.
898 [47] J. Dhont, Chromatographic behavior of 2, 4-dinitrophenylhydrazones on
899 chromatoplates, Royal Soc Chemistry Thomas Graham House, Science park, Milton
900 Rd, Cambridge CB4 0WF, Cambs, England, 1961, pp. 74-&.
901 [48] T.N. Corso, B.A. Lewis, J.T. Brenna, Reduction of Fatty Acid Methyl Esters to
902 Fatty Alcohols To Improve Volatility for Isotopic Analysis without Extraneous
903 Carbon, Analytical Chemistry, 70 (1998) 3752-3756.
904 [49] T.N. Corso, J.T. Brenna, On-line pyrolysis of hydrocarbons coupled to high-
905 precision carbon isotope ratio analysis, Analytica Chimica Acta, 397 (1999) 217-224.
906 [50] C.J. Wolyniak, G.L. Sacks, S.K. Metzger, J.T. Brenna, Determination of
907 Intramolecular delta13C from incomplete pyrolysis fragments. Evaluation of
908 pyrolysis-induced isotopic fractionation in fragments from the lactic acid analogue
909 propylene glycol, Anal Chem, 78 (2006) 2752-2757.
910 [51] W.F. Maier, W. Roth, I. Thies, P.V.R. Schleyer, Hydrogenolysis, IV. Gas phase
911 decarboxylation of carboxylic acids, Chemische Berichte, 115 (1982) 808-812.
912 [52] T.N.C. J.T.Brenna, H.J.Tobias, R.J.Calmi, High-precision continuous-flow
913 isotope ratio mass spectrometry, Mass Spectrometry Reviews, 16 (1997) 227-258.
914 [53] J.M. Eiler, The Isotopic Anatomies of Molecules and Minerals, Annu Rev Earth
915 Pl Sc, 41 (2013) 411-441.
916 [54] K. Yamada, M. Kikuchi, A. Gilbert, N. Yoshida, N. Wasano, R. Hattori, S.
917 Hirano, Evaluation of commercially available reagents as a reference material for
918 intramolecular carbon isotopic measurements of acetic acid, Rapid Communications
919 in Mass Spectrometry, 28 (2014) 1821-1828.
920

Table 1-

Stable Isotope Analysis	Details	Example	Techniques
Bulk Isotope Analysis (BSIA)	Weighted average isotopic signature of the components of the sample	δ^{13}C of gasoline samples 	• Off-line transformation of the sample gases and analysis in dual inlet IRMS • Continuous flow EA-IRMS/TC EA-IRMS
Compound Specific Isotope Analysis (CSIA)	Isotopic signatures of the individual compounds of a mixture- *Inter*molecular isotopic variations	δ^{13}C of individual compounds of gasoline such as methyl *tert* butyl ether, ethyl *tert butyl* ether, benzene, toluene, xylenes 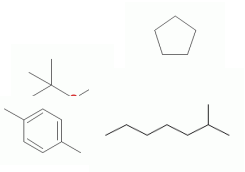	• Off-line extraction of a mixture and analysis by EA-IRMS TC/EA-IRMS • Continuous Flow GC-IRMS
Position Specific Isotope Analysis (PSIA)	Isotopic signatures of different moieties in a molecule- *Intra*molecular isotopic variations	δ^{13}C of the two methyl *tert* butyl ether moieties 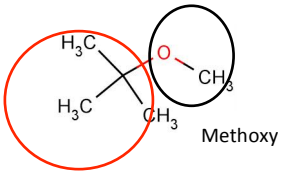 Methoxy 2-methylpropyl	• Off-line transformation of a functional group into a simple gas (CO_2) and analysis by dual inlet IRMS • Off-line breakdown (chemolysis, pyrolysis) of a molecule and analysis by GC-IRMS of the fragments • SNIF-NMR • **On-line PSIA using CF-IRMS**

Type of Compounds	Compound	Fragmentation Products	Fragmentation Mechanisms	Optimum Fragmentation Temperature	f[1]	Secondary Reactions	100% Fidelity[2]	System[3]	Ref
Simple fragmentation of small molecules	Benzoic acid	Benzene and carbon dioxide	Decarboxylation	750˚C	n.r.	No	Yes	1	[44]
	Napthylactic acid	Naphthalene and carbon dioxide	Decarboxylation	750˚C	n.r.	No	Yes	1	[44]
	1-Pyrenecarboylic acid	Pyrene and carbon dioxide	Decarboxylation	750˚C	n.r.	No	Yes	1	[44]
	Acetic acid	Methane and carbon dioxide	Decarboxylation	600˚C	n.r.	No	Yes	2	[45]
	Acetic acid	Methane and carbon dioxide	Pd-catalysed Decarboxylation with hydrogen	960˚C	n.r.	No	Yes	3	[22]
	Methyl *tert* butyl ether	Methanol and isobutylene	Pyrolysis: Cleavage of the C-O bond by intramolecular elimination	675˚C	7-40%	Yes	Yes	5	[29]
	Ethanol	Carbon monoxide, methane, water and ethylene	Pyrolysis 1) Dehydration 2) Cleavage of the C-C bond.	1000˚C	<5%	Yes	Yes	3	[23]
	Toluene	Benzene and methane	Pyrolysis Cleavage of the C-C bond between the benzene ring and the methyl group of toluene	800˚C	97%	Yes	Yes	4	[49]
Non-ideal fragmentation of small molecules	Analogue of Phenylalanine: phenethylamine	Benzene and toluene	Pyrolysis Cleavage of the C-C bond at the benzene ring Scrambling	900˚C	n.r.	No	No	4	[25]
	Analogue of Alanine: Alaninol	Carbon monoxide, methane, ethylene, ethane, propylene and acetonitrile	Pyrolysis Cleavage on the methane, amine and alcohol fragments Scrambling	900˚C	n.r.	No	No	4	[25]
	Decarboxylated analogue of Methionine: Isoamylamine	Propylene, isobutylene, hydrogen cyanide, acetonitrile	Pyrolysis Cleavage on the methane and amine fragments Scrambling	780˚C	6%	Yes	No	4	[24]
	Decrboxylated analogue of Leucine: 3-methylthiopropylamine	Methane, ethane, hydrogen cyanide, acetonitrile	Pyrolysis Cleavage on the methane, amine and sulphide fragments Scrambling	880˚C	n.r.	Yes	No	4	[24]
	Lactic acid analogue: Propylene glycol	Methanol, methane, ethylene, acetaldehyde, propylene, ethanol, propanol	Pyrolysis Cleavage on the methane and alcohol fragments Scrambling	700˚C	66%	No	No	4	[50]
Pyrolysis of long chain molecules	n-alkanes	α olefin series and ω - unsaturated alcohol series	Pyrolysis Cleavage of a single C-C bond and the formation of complementary fragments	550˚C	n.r.	No	Yes	4	[49]
	Hexadecanol	α olefin series and ω - unsaturated alcohol series	Pyrolysis Cleavage of a single C-C bond and the formation of complementary fragments	600˚C	n.r.	No	Yes	4	[48]
	FAMEs: Methylpalmitate	methyl ester mono unsaturated and α olefin series	Pyrolysis Cleavage of a single C-C bond and the formation of complementary fragments	550˚C	80%	No	Yes	4	[3]

System[1]	Reported Precision	Reported Sensitivity	Ref
1	1σ= 0.4‰. Instrumentation precision for the carboxylic carbon	Analysis was carried out with <3µmol of sample on column ≈200 nmol C	[44]
2	1σ=0.7‰ Instrumentation precision for the carboxylic carbon	Not reported	[45]
3	1σ=0.4‰ Instrumentation precision	Analysis was carried out with 11.5 nmol of acetic acid on the column - 23 nmol C	[22]
4	2σ≈0.4‰ for $\Delta\delta^{13}C$ (*spl*) of pyrolysates 1σ <3.0‰ for $\Delta\delta^{13}C$ of moieties.	Analysis carried out with 2 to 4 µg of sample on the column. Sensitivity was limited by the yield of the pyrolysis.	[3] [25]
5	95% confidence = 0.5‰ for $\delta^{13}C_{VPDB}$ values of the two MTBE moieties.	Sensitivity diminished by the addition of helium in the system and the presence of the open-split and limited by the yield of the pyrolysis.	[29]

Figure 1

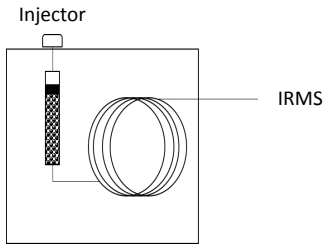

System 1 [44]

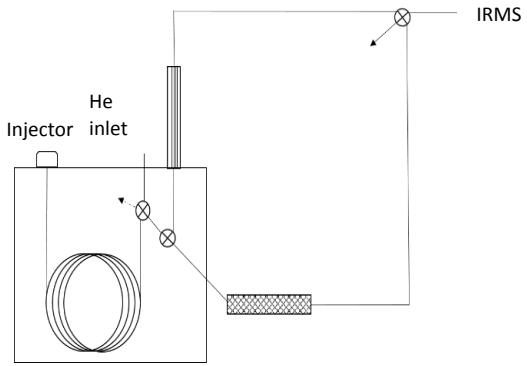

System 2 [45]

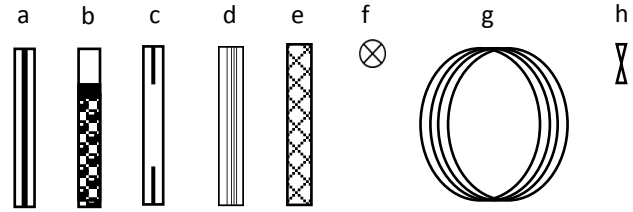

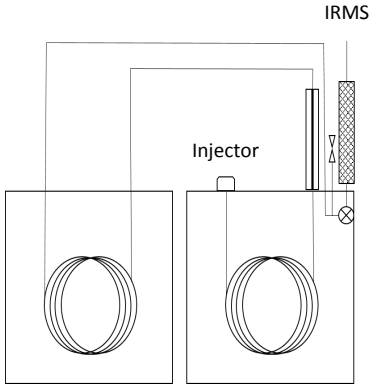

System 3 [22]

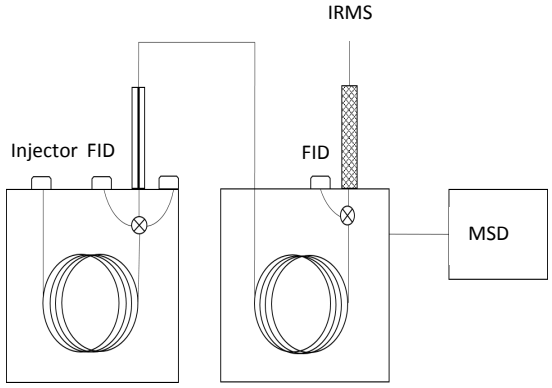

System 4 [3]

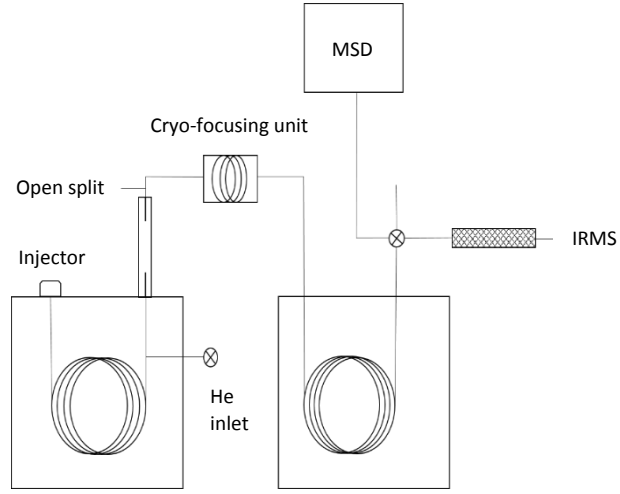

System 5 [29]

Figure 2

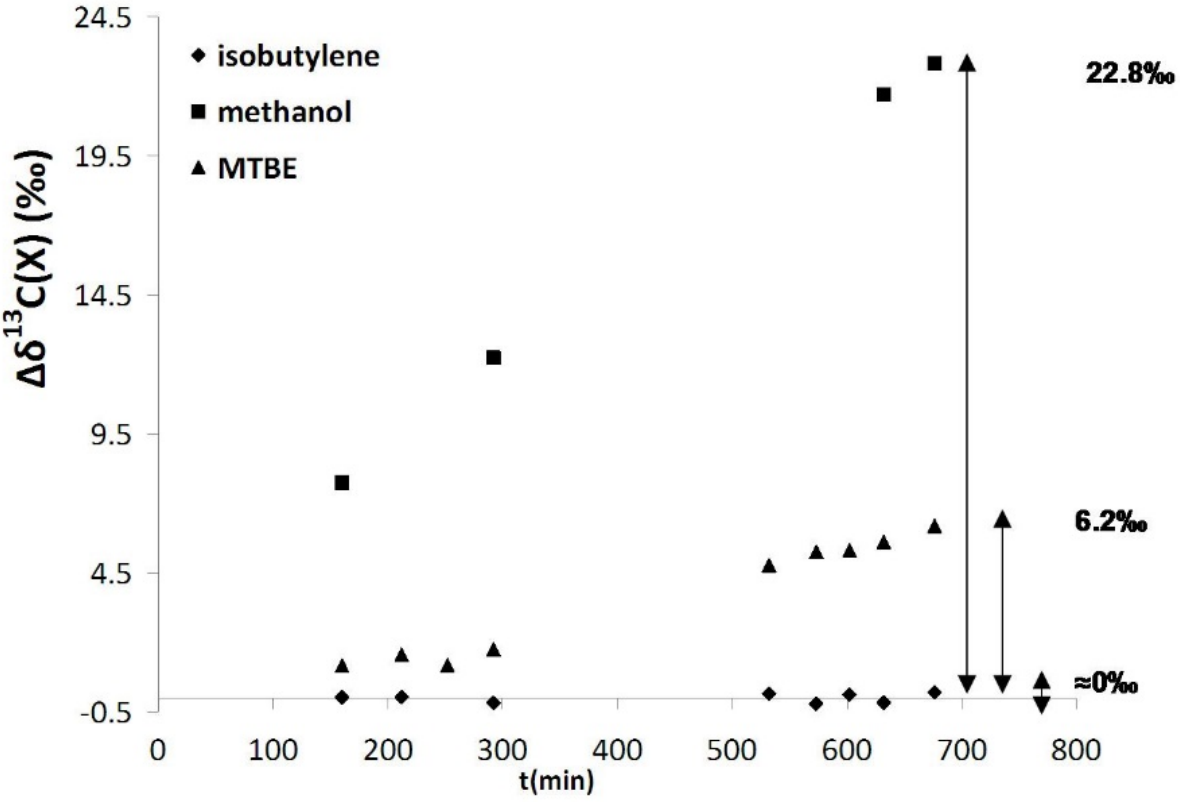
24.5
19.5
14.5
9.5
4.5
-0.5
0
100
200
300
400
500
600
700
800
t(min)
$\Delta\delta^{13}C(X)$ (‰)
isobutylene
methanol
MTBE
22.8‰
6.2‰
≈0‰